Anomerisation of fluorinated sugars by mutarotase studied by ^{19}F NMR two-dimensional exchange spectroscopy

Dmitry Shishmarev[a], Lucas Quiquempoix[b], Clément Q. Fontenelle[b], Bruno Linclau[b], and Philip W. Kuchel[c*]

[a]*John Curtin School of Medical Research, Australian National University, ACT, Australia*

[b]*School of Chemistry, University of Southampton, Southampton, UK*

[c]*School of Life and Environmental Sciences, University of Sydney, NSW, Australia*

Running heading: Mutarotase and fluorinated sugars

***Correspondence**: Philip W. Kuchel
School of Life and Environmental Sciences
Building G08
University of Sydney
New South Wales, 2006
Australia
Email: philip.kuchel@sydney.edu.au
Fax: (02) 9351 4726

Keywords: 2D exchange spectroscopy; fluorinated glucose; mutarotase; NMR; enzyme inhibition; enzyme mechanism

Abbreviations: 1D, one-dimensional; 2D, two-dimensional; FDG2, 2-fluoro-2-deoxy-D-glucose; FDG23, 2,3-difluoro-2,3-dideoxy-D-glucose; FDG2233, 2,2,3,3-tetrafluoro-2,3-dideoxy-D-glucose; FDG3, 3-fluoro-3-deoxy-D-glucose; FDG4, 4-fluoro-4-deoxy-D-glucose; NMR, nuclear magnetic resonance; RBC, red blood cell; 2D-EXSY, two-dimensional exchange spectroscopy;

Abstract

Five ^{19}F-substituted glucose analogues were used to probe the activity and mechanism of the enzyme mutarotase by using magnetisation-exchange NMR spectroscopy. The sugars [2-fluoro-2-deoxy-D-glucose, FDG2; 3-fluoro-3-deoxy-D-glucose, FDG3; 4-fluoro-4-deoxy-D-glucose, FDG4; 2,3-difluoro-2,3-dideoxy-D-glucose, FDG23; and 2,2,3,3-tetrafluoro-2,3-dideoxy-D-glucose (2,3-dideoxy-2,2,3,3-tetrafluoro-D-*erythro*-hexopyranose), FDG2233] showed separate ^{19}F NMR spectral resonances from their respective α- and β-anomers, thus allowing two-dimensional exchange spectroscopy measurements of the anomeric interconversion at equilibrium, on the time scale of a few seconds. Mutarotase catalysed the *rapid* exchange between the anomers of FDG4, but not the other four sugars. This finding, combined with previous work identifying the mechanism of the anomerisation by mutarotase, suggests that the rotation around the C1-C2 bond of the pyranose ring is the rate-limiting reaction step. In addition to D-glucose itself, it was shown that all other fluorinated sugars inhibited the FDG4 anomerisation, with the tetrafluorinated FDG2233 being the best inhibitor. Inhibition of mutarotase by F-sugars paves the way for development of novel fluorinated compounds that are able to affect the activity of this enzyme *in vitro* and *in vivo*.

Introduction

Mutarotase (aldose 1-epimerase; EC. 5.1.3.3) is the enzyme that catalyses the interconversion between two anomeric forms of several monosaccharides, reactions that usually occurs on a time scale of several minutes/hours in the absence of the enzyme (see the previous paper in this Special Edition). The human mutarotase was initially purified from erythrocytes (red blood cells; RBCs) in the 1960s[1-2] where, paradoxically, its activity is relatively low.[3] In fact, the highest activities of the enzyme in mammalian tissues have been reported in the kidney[4] and the corresponding gene was identified and cloned in 2003.[5]

Mutarotase is known to play an important role in the Leloir pathway of catabolism of D-galactose, by enhancing the rate of interconversion between the two sugar anomers. This is critical for some organisms because only α-D-galactose is processed by the next enzyme in the pathway, galactokinase (EC 2.7.1.6).[6-7] Thus, despite spontaneous mutarotation, the enzyme is required for efficient catabolism of lactose by *E. coli*; and strains with a 'restrictive' mutation in their mutarotase gene grow more slowly in cultured minimal media.[8] Hence, it is of clinical interest to develop novel inhibitors of mutarotase, as they might have use as antimicrobial agents, and to probe various aspects of the "metabolic subculture" of sugars. (See the previous paper in this Special Edition for a general discussion of this topic.)

Kinetic assays

The classical way of conducting kinetic assays of mutarotase is to start the reaction with one of the anomeric forms of a monosaccharide and monitor the reaction by recording changes in optical rotation with a polarimeter.[2, 9] Alternatively, the mutarotation reaction can be coupled with that of another enzyme that selectively processes only one anomeric form of the sugar. In that case, the activity of the latter enzyme can be quantified by other methods, such as spectrophotometry, and it will indirectly report on the activity of mutarotase. Examples of coupling enzymes include galactose 1-dehydrogenase (EC 1.1.1.48) and glucose 1-dehydrogenase (EC 1.1.1.47).[5]

In contrast to the assays based on polarimetry or optical absorption measurements, NMR methodology is unique in that it allows simultaneous monitoring of the anomerisation reactions of several sugars in a mixture, even under equilibrium-exchange conditions. Previous NMR-based studies of sugar anomerisation include those using ^{1}H NMR[10] and ^{13}C NMR of ^{13}C-labelled glucose.[3, 11] The latter study has been the most detailed: the rates of exchange between the α- and β-anomers of [1,^{13}C]D-glucose catalysed by porcine kidney mutarotase (as used for

the present work) have been measured using several ^{13}C NMR magnetisation-transfer procedures.[11] These involved one-dimensional (1D) inversion- and saturation-transfer experiments as well as two-dimensional (2D) exchange spectroscopy (EXSY). The concentration and temperature dependence of the reaction fluxes were measured and estimates of the Michaelis-Menten steady-state kinetic constants and the activation energy of the catalysed reaction were made. These previous studies guided the present work by providing information on sample preparation as well as NMR and computational foundations for studying the kinetics of mutarotase using 2D-EXSY.

Aims and motivation

^{19}F-substituted monosaccharide analogues have been reported as probes to study protein-carbohydrate interactions,[12-13] including via ^{19}F NMR experiments.[14] In addition, ^{19}F NMR exchange spectroscopy has been employed in the context of their interaction with the glucose transporter GLUT1 in erythrocytes.[15-22] The main aim of the present work was to study the anomerisation of five fluorine-substituted glucoses (Fig. 1) in the presence of mutarotase by using ^{19}F NMR 2D-EXSY. This was pursued with a view to identifying those sugar derivatives that might be useful for inhibiting this enzyme *in vivo* and/or used in NMR-spectroscopic imaging of the kidney and other organs, as outlined in the previous paper in this Special Edition. Additionally, the analysis would elaborate on the contemporary understanding of the molecular mechanism of the operation of this enzyme. To our knowledge, this is the first time that anomerisation of ^{19}F-substituted glucose analogues by mutarotase has been studied.

Results

1D ^{19}F NMR spectra

Figure 1 shows the molecular structures of the fluorinated analogues of glucose that were used in this study: 2-fluoro-2-deoxy-D-glucose (FDG2), 3-fluoro-3-deoxy-D-glucose (FDG3), 4-fluoro-4-deoxy-D-glucose (FDG4), 2,3-difluoro-2,3-dideoxy-D-glucose (FDG23), and 2,2,3,3-tetrafluoro-2,3-dideoxy-D-glucose (2,3-dideoxy-2,2,3,3-tetrafluoro-D-*erythro*-hexopyranose, FDG2233).

First, we used 1D ^{19}F NMR spectroscopy to check the purity of the studied F-substituted glucoses and to record reference spectra for the subsequent 2D-EXSY measurements. The relevant regions of the 1D ^{19}F NMR spectrum of a mixture of FDG2, FDG3, FDG4, FDG23 and FDG2233 in the presence of mutarotase are shown in Figure 2. The ^{19}F NMR assignments,

indicated in Fig. 2, were conducted on the basis of previously published reports.[10, 22-24] Interestingly, the two diastereotopic fluorine atoms of FDG2233 at the 3-position display a similar chemical shift value for both anomers. Each of the sugars showed separate resonances from their α- and β-anomers. This opened up the possibility of studying the rates of their anomerisation by 2D-EXSY ^{19}F NMR.

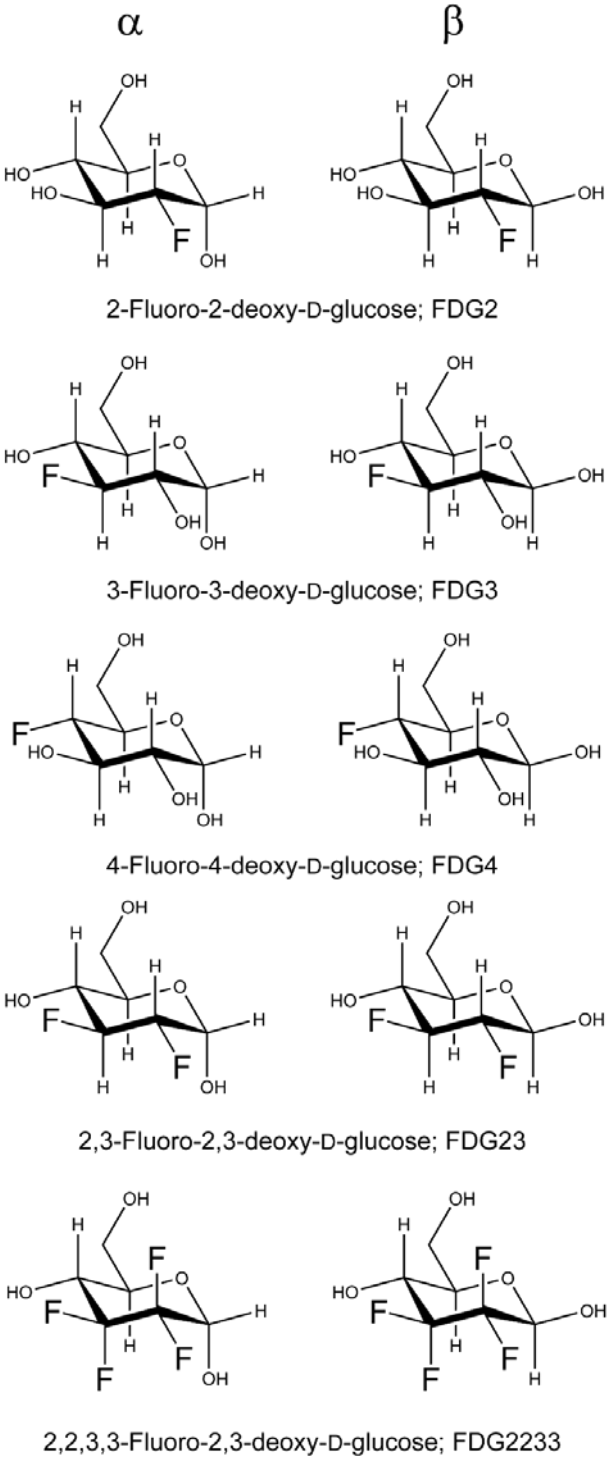

Fig. 1. Molecular structures of the F-substituted glucose analogues used in the present study.

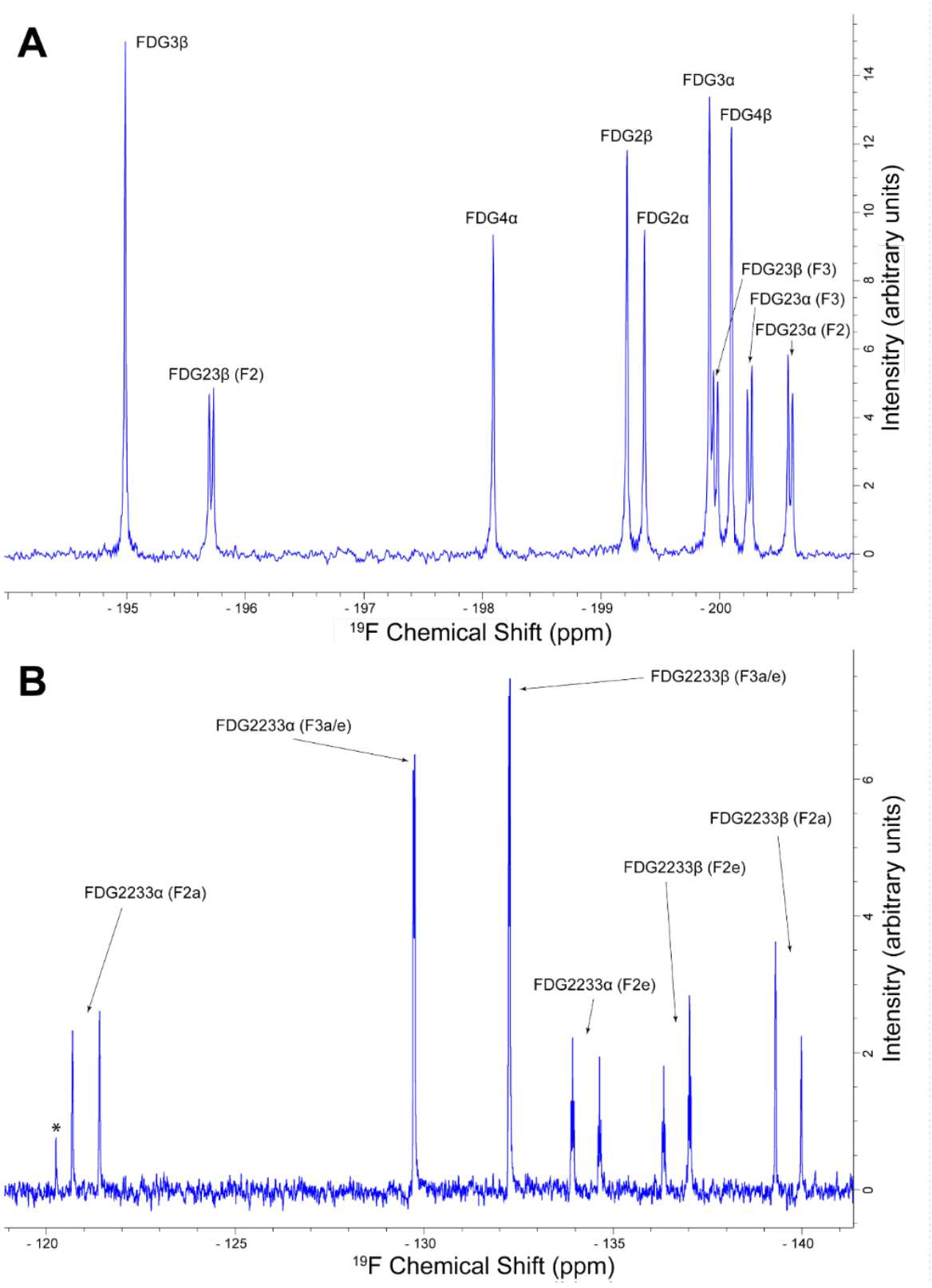

Fig. 2. 1D ^{19}F NMR spectrum of a mixture of 10 mM FDG2, 10 mM FDG3, 10 mM FDG4, 8 mM FDG23 and 8 mM FDG2233 in the presence of porcine kidney mutarotase (0.181 mg mL^{-1}). Buffer: 20 mM Na_2HPO_4, 127 mM NaCl, 0.1 mM EDTA, 0.1 mM DTT and 10% D_2O (pH 7.4). (**A**) Spectral region showing resonances of FDG2, FDG3, FDG4 and FDG23. (**B**) Spectral region showing resonances of FDG2233. * indicates the resonance from an unassigned impurity in the FDG2233 sample.

The equilibrium constant of the anomerisation reaction, K_{eq}, for each of the investigated FDGs was calculated from the ratio of the integrals of the resonances (proportional to concentrations), corresponding to α- and β-anomers in the 1D NMR spectrum (Fig. 2):

$$K_{eq} = \frac{[\beta]_{eq}}{[\alpha]_{eq}} \quad (1)$$

where $[\alpha]_{eq}$ and $[\beta]_{eq}$ are the concentrations of the respective anomers at equilibrium. For each of the investigated sugars, the measured chemical shifts, *J* coupling constants, peak integrals and K_{eq} values are given in Table 1.

Table 1. Values of the chemical shifts, *J* coupling constants, peak integrals and anomerisation equilibrium constants K_{eq} for each of the investigated fluorinated sugars, measured from the 1D ^{19}F NMR spectrum of Fig. 2.

F-sugar	**Anomer**	**^{19}F chemical shift (ppm) and *J* coupling values (Hz)**	**Peak integral (arbitrary units)[a]**	**K_{eq}**
FDG2	α	-199.37 (1F, s)	118.034	1.25
	β	-199.22 (1F, s)	148.072	
FDG3	α	-199.91 (1F, s)	165.816	1.09
	β	-194.99 (1F, s)	180.038	
FDG4	α	-198.09 (1F, s)	115.991	1.36
	β	-200.10 (1F, s)	157.265	
FDG23	α	-200.25 (1F, d, *J* 13.8, F3)	117.200	0.90
		-200.60 (1F, d, *J* 13.9, F2)	122.675	
	β	-195.71 (1F, d, *J* 13.6, F3)	112.740	
		-199.96 (1F, d, *J* 13.5, F2)	103.998	
FDG2233	α	-121.05 (1F, d, *J* 268.9, F2a)	118.868	1.04
		-129.73 (2F, d, *J* 13.2, F3a/e)	230.340	
		-134.29 (1F, dt, *J* 269.1 and 13.3, F2e)	103.658	
	β	-132.26 (2F, d, *J* 12.4, F3a/e)	235.370	
		-136.68 (1F, dt, *J* 257.8 and 12.8, F2e)	110.490	
		-139.64 (1F, d, *J* 257.9, F2a)	123.779	

[a]The number of significant digits recorded here exceeds the number of actual significant digits; however, they were retained to obviate rounding errors in the subsequent calculations of K_{eq} values.

The 1D ^{19}F NMR spectra attested to the high purity of the synthetic products. However, there was a minor admixture in the FDG2233 sample indicated by a small peak at -120.255 ppm (marked by * in Fig. 2). Even though furanose forms of some of the sugar phosphates have been encountered in ^{31}P NMR spectra of pentose phosphate pathway intermediates,[25] no furanose forms were visible for any of the sugars in the present work.

2D-EXSY

Next, we employed 2D-EXSY methodology to reveal whether mutarotase is able to catalyse the anomerisation of any of the studied fluorinated sugars. Figure 3 shows 2D-EXSY spectra of each individual fluorinated sugar in the presence of mutarotase, obtained with a mixing time $t_{mix} = 2$ s. For each of the peaks in the 1D ^{19}F NMR reference spectrum (Fig. 2), a corresponding diagonal peak, with the same chemical shift in each dimension, is marked in the 2D-EXSY spectra (Fig. 3). For FDG2, FDG3 and FDG23, there were no cross-peaks in the spectra (Fig. 3A-C). For FDG2233, there were cross-peaks between the two components of the doublets, split by the large geminal ^{19}F-^{19}F coupling, thus these were not the 'true' exchange cross-peaks that would indicate anomerisation (Fig. 3D). Interestingly, only for FDG4 were there exchange cross-peaks between the two anomeric species (two peaks labelled as 'FDG4α/β' and 'FDG4β/α' in Fig. 3E), indicating rapid mutarotaion of this sugar in the presence of the enzyme.

In order to check whether mutarotase becomes completely deactivated by the presence of any of the studied F-sugars, thus leading to the absence of cross-peaks in the 2D-EXSY spectra (Fig. 3A-D), we prepared a sample containing a mixture of all the studied fluorinated sugars and repeated the 2D-EXSY measurements. Figure 4 shows 2D-EXSY ^{19}F NMR spectra of a mixture of FDG2, FDG3, FDG4, FDG23, and FDG2233 (same sample as used for the spectrum of Fig. 2). Again, as in the experiments of Fig. 3, only FDG4 displayed the exchange cross-peaks between α- and β-anomer (Fig. 4). Thus, mutarotase remains active in the presence of any of the F-sugars used in this work. However, as there were no exchange cross-peaks for FDG2, FDG3, FDG23, and FDG2233, it is clear that mutarotase only catalysed interconversion between the two anomers of FDG4, and no other studied F-sugars (at least on the time scale of the 2-s mixing time).

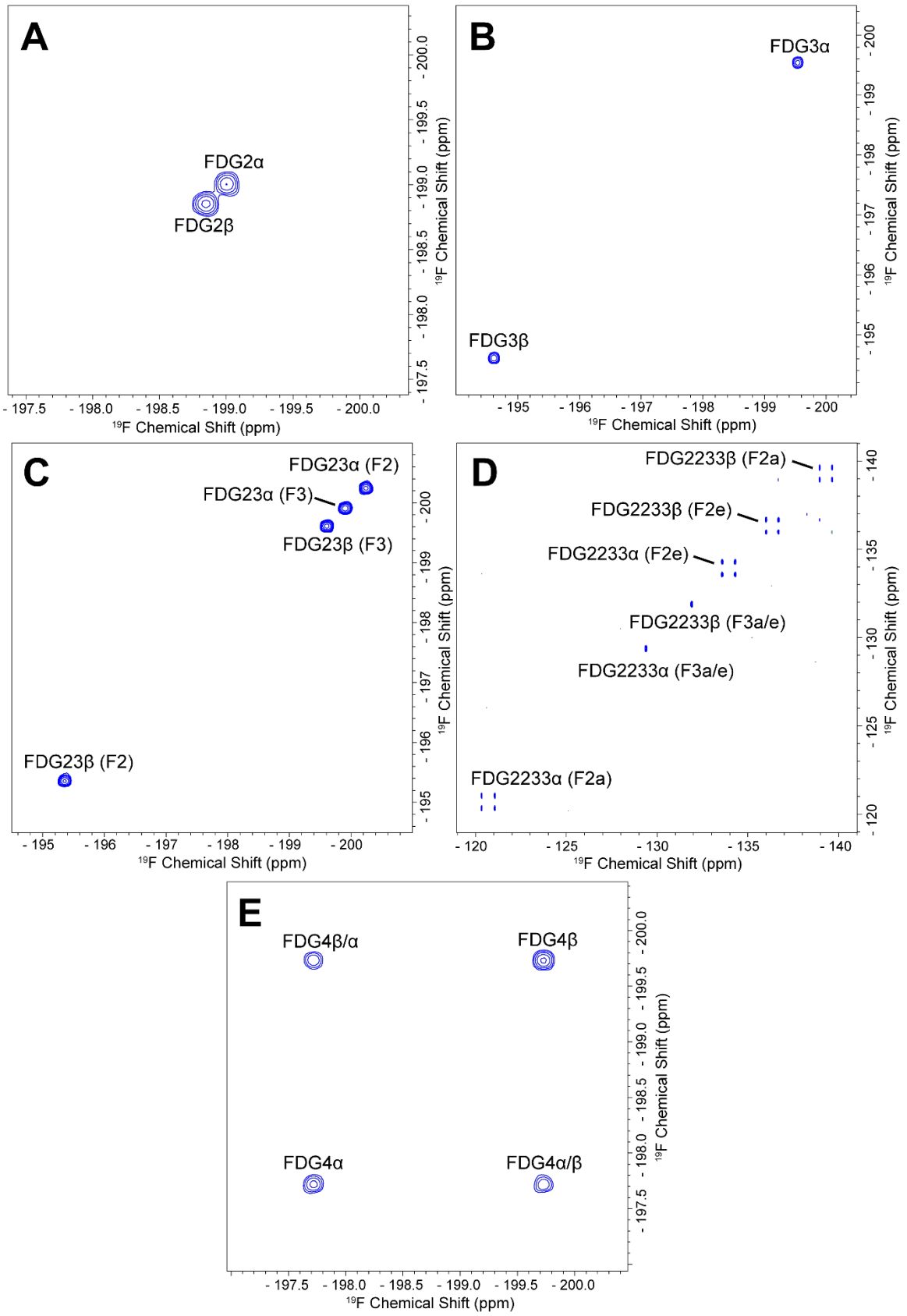

157

158 **Fig. 3.** 2D-EXSY ^{19}F NMR spectra of individual fluorinated sugars (at 5 mM concentrations) in the presence of
159 mutarotase (0.046 mg mL^{-1}). Mixing time, 2 s. Buffer: 20 mM Na_2HPO_4, 127 mM NaCl, 0.1 mM EDTA, 0.1 mM
160 DTT and 10% D_2O (pH 7.4). (**A**) FDG2, (**B**) FDG3, (**C**) FDG23, (**D**) FDG2233, (**E**) FDG4.

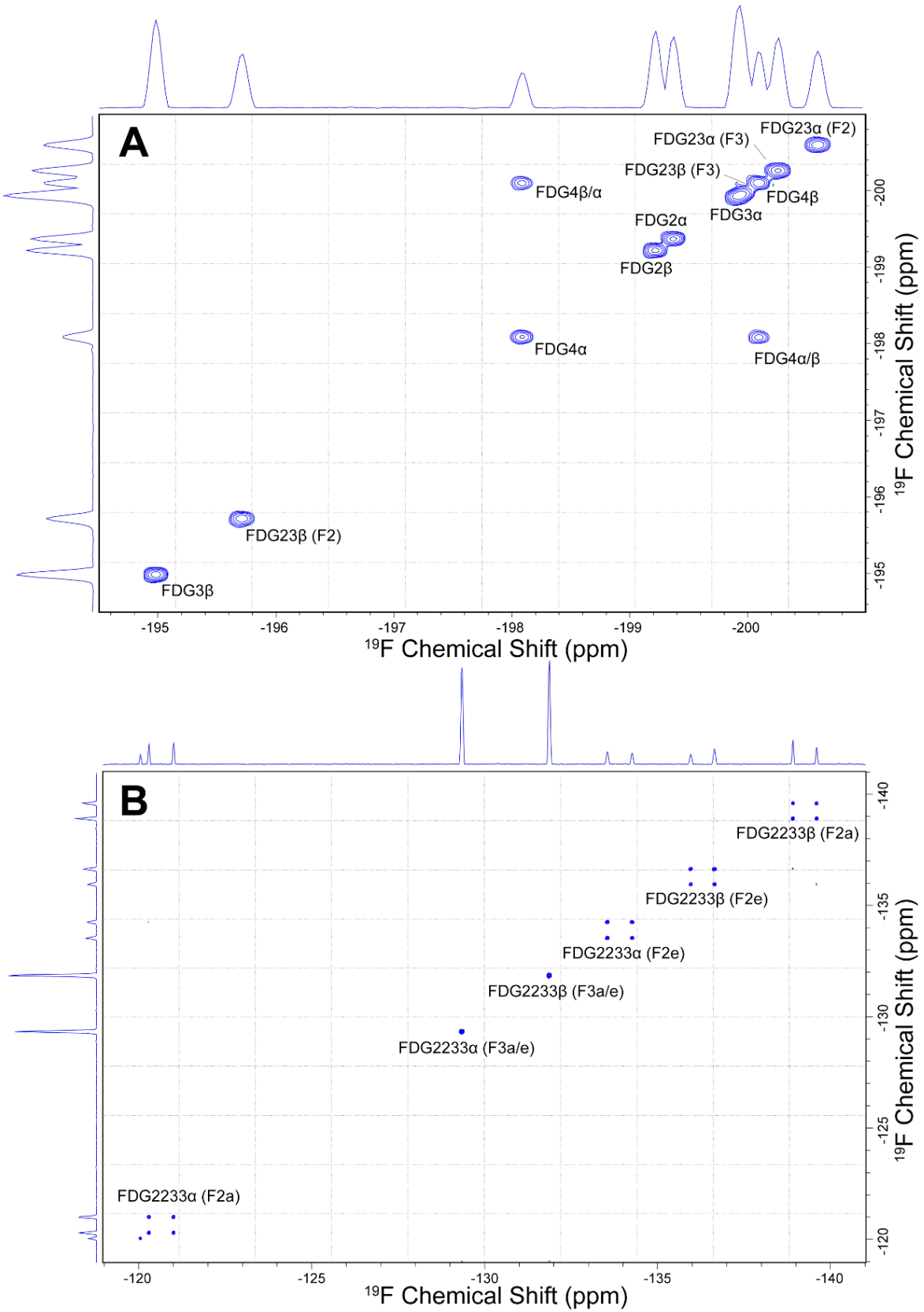

Fig. 4. 2D-EXSY ^{19}F NMR spectra of a mixture of 10 mM FDG2, 10 mM FDG3, 10 mM FDG4, 8 mM FDG23 and 8 mM FDG2233 in the presence of mutarotase (0.181 mg mL^{-1}). Mixing time, 2 s. Buffer: 20 mM Na_2HPO_4, 127 mM NaCl, 0.1 mM EDTA, 0.1 mM DTT and 10% D_2O (pH 7.4). (**A**) Spectral region showing resonances of FDG2, FDG3, FDG4 and FDG23. (**B**) Spectral region showing resonances of FDG2233.

Different mutarotase concentrations

In order to establish that the observed anomerisation of FDG4 is indeed catalysed by mutarotase (and is not spontaneously rapid in its own right), we recorded a series of 2D-EXSY spectra of FDG-4 in the presence of various amounts of mutarotase (Fig. 5). In the complete absence of mutarotase, the exchange cross-peaks did not appear (Fig 5; black spectrum). Next, as the concentration of mutarotase was increased in the NMR sample from 0 up to 0.174 mg mL^{-1}, the exchange peaks steadily grew in intensity (Fig. 5). Thus, the observed rapid anomerisation of FDG4 was indeed catalysed by mutarotase, and the contribution of the spontaneous mutarotation in the conducted experiments was negligible.

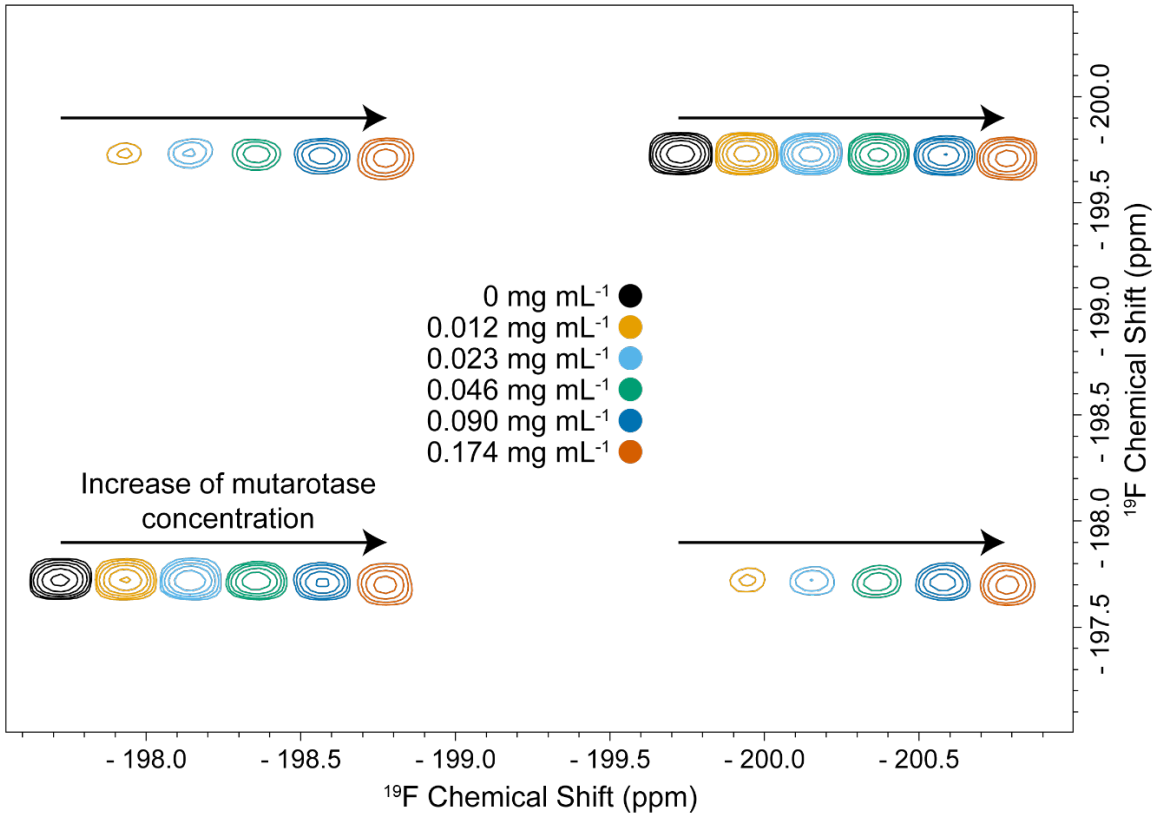

Fig. 5. 2D-EXSY ^{19}F NMR spectra of 10 mM FDG4 in the presence of different quantities of mutarotase (0, 0.012, 0.023, 0.046, 0.090, and 0.174 mg mL^{-1}, as indicated in the figure legend). Buffer: 20 mM Na_2HPO_4, 127 mM NaCl, 0.1 mM EDTA, 0.1 mM DTT and 10% D_2O (pH 7.4). For clarity, the spectra (apart from the black one) were shifted horizontally with respect to each other.

Back-transformation analysis

Quantification of the rate of FDG4 mutarotation, based on the 2D-EXSY spectra, employed the 'back-transformation' method that provides estimates of the unidirectional *apparent* rate constants $k_{\alpha\beta}$ and $k_{\beta\alpha}$ for the reversible anomerisation reaction (Scheme 1).[26]

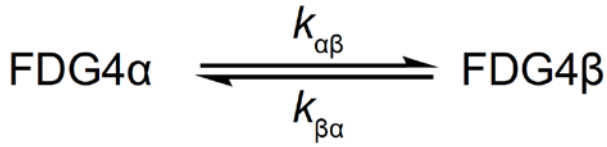

Scheme 1. Kinetic scheme of the anomerisation of FDG4 under equilibrium-exchange conditions.

At chemical equilibrium, the rate of the forward reaction is equal to the rate of the reverse reaction:

$$k_{\alpha\beta}[\alpha]_{eq} = k_{\beta\alpha}[\beta]_{eq} \quad (2)$$

Combining Eqs. 1 and 2 shows that the apparent rate constants are related to the equilibrium constant:

$$\frac{k_{\alpha\beta}}{k_{\beta\alpha}} = K_{eq} \quad (3)$$

During the mixing-time period of the 2D-EXSY experiment, the dependence of the integrals of the four peaks assigned to FDG4 (two diagonal peaks and two cross-peaks; Fig. 3E) is described by the Bloch-McConnell differential equations in matrix form:[11, 26-27]

$$\frac{d\boldsymbol{I}(t)}{dt} = \boldsymbol{R} \cdot \boldsymbol{I}(t) \quad (4)$$

where $\boldsymbol{I}(t)$ and $\boldsymbol{R}$ are 2 × 2 matrices; the former is composed of four integral values, while the latter is formed as a combination of the longitudinal relaxation rate constants and the exchange rate constants:

$$\boldsymbol{I}(t) = \begin{bmatrix} I_{\alpha\alpha}(t) & I_{\beta\alpha}(t) \\ I_{\alpha\beta}(t) & I_{\beta\beta}(t) \end{bmatrix} \quad (5)$$

$$\boldsymbol{R} = \begin{bmatrix} -\frac{1}{T_1^{\alpha}} - k_{\alpha\beta} & k_{\beta\alpha} \\ k_{\alpha\beta} & -\frac{1}{T_1^{\beta}} - k_{\beta\alpha} \end{bmatrix} \quad (6)$$

where, for FDG4, the variables $I_{\alpha\alpha}(t)$, $I_{\beta\beta}(t)$, $I_{\alpha\beta}(t)$, and $I_{\beta\alpha}(t)$ denote the time-dependent values of the integrals of the peaks labelled in Fig. 3E as 'FDG4α', 'FDG4β', 'FDG4α/β' and

'FDG4β/α', respectively; while T_1^{α} and T_1^{β} are the respective longitudinal relaxation time constants for FDG4α and FDG4β.

Integration of the matrix differential equation gives the following analytical solution:

$$\boldsymbol{I}(t) = \boldsymbol{I}(0)\exp(\boldsymbol{R}t) \quad (7)$$

Calculating the elements of the matrix $\boldsymbol{R}$ is carried out by using the back-transformation formula, at a time $t = t_{\mathrm{mix}}$:

$$\boldsymbol{R} = \frac{\ln[\boldsymbol{I}(0)^{-1} \cdot \boldsymbol{I}(t_{\mathrm{mix}})]}{t_{\mathrm{mix}}} \quad (8)$$

where $\boldsymbol{I}(0)^{-1}$ is the inverse of the matrix $\boldsymbol{I}(0)$ and the natural logarithm of a matrix can be taken after its diagonalisation.[28]

As shown previously,[26] if only the rate-constant estimates are of interest, a 2D-EXSY spectrum with zero mixing time is not needed to obtain the matrix $\boldsymbol{I}(0)$. Instead, this matrix is constructed, as follows:

$$\boldsymbol{I}(0) = \begin{bmatrix} I_{\alpha} & 0 \\ 0 & I_{\beta} \end{bmatrix} \quad (9)$$

where I_{α} and I_{β} are the peak integrals corresponding to FDG4α and FDG4β in the 1D ^{19}F NMR spectrum. This is the insight that was used in the present work.

Rate dependence on enzyme concentration

Thus, quantification of the anomerisation kinetics of FDG4 was based on measuring peak integrals of these 2D-EXSY ^{19}F NMR spectra, and applying the back-transformation procedure (Eq. 8) in order to estimate the non-diagonal elements of matrix, $\boldsymbol{R}$.[26] Table 2 summarises the apparent rate constant of the anomerisation reaction of FDG4, estimated from the 2D-EXSY spectra of Fig. 4.

Table 2. Values of the apparent rate constants $k_{\alpha\beta}$ and $k_{\beta\alpha}$ of 10 mM FDG4, estimated from the 2D-EXSY spectra of Fig. 4, for each of the studied mutarotase concentrations.

Mutarotase concentration (mg mL^{-1})	$\boldsymbol{k_{\alpha\beta}}$ **(s^{-1})**	$\boldsymbol{k_{\beta\alpha}}$ **(s^{-1})**
0	0	0
0.012	0.04 ± 0.01	0.05 ± 0.01

0.023	0.07 ± 0.01	0.10 ± 0.01
0.046	0.11 ± 0.01	0.15 ± 0.01
0.090	0.29 ± 0.01	0.41 ± 0.01
0.174	0.49 ± 0.02	0.67 ± 0.03

The dependencies of the apparent rate constants of FDG4 mutarotation on the mutarotase concentration were plotted (Fig. 6), and a linear model was fitted to these data with coefficients of determination close to 1 ($R^2 = 0.991$ and $R^2 = 0.987$ for $k_{\alpha\beta}$ and $k_{\beta\alpha}$, respectively). This indicated a linear dependence of the apparent rate constants on the enzyme concentration (in the studied concentration range up to 0.174 mg mL^{-1}).

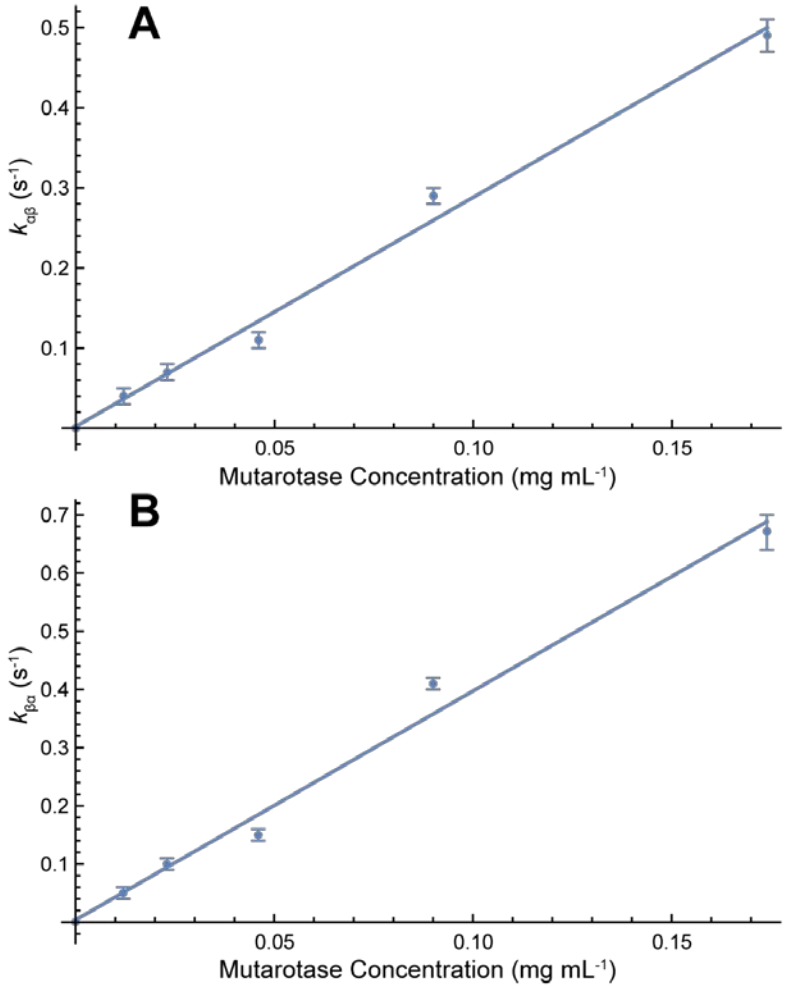

Fig. 6. Dependence of the apparent rate constants of mutarotation of 10 mM FDG4, estimated from the 2D-EXSY spectra of Fig. 5, on the mutarotase concentration. Experimental points are shown as circles with the associated error bars, while the solid lines are linear-regression fits. (**A**) $k_{\alpha\beta}: y = 2.861\,x + 0.002; R^2 = 0.991$. (**B**) $k_{\beta\alpha}: y = 3.935\,x + 0.004; R^2 = 0.987$.

Inhibition of mutarotase by D-glucose and FDGs

In order to probe the mechanism of FDG4 interaction with the mutarotase, we tested whether a natural substrate, D-glucose, competes with FDG4 for the anomerisation reaction. We recorded 2D-EXSY spectra of 10 mM FDG4 in the presence of mutarotase and various amounts of D-glucose. The 2D-EXSY spectra are shown in Fig. 7. There was little change in the spectra at D-glucose concentrations within the range 0-20 mM. However, upon addition of 100 mM, and especially 250 mM D-glucose, the exchange peaks significantly reduced in intensity, indicating slower anomerisation of FDG4.

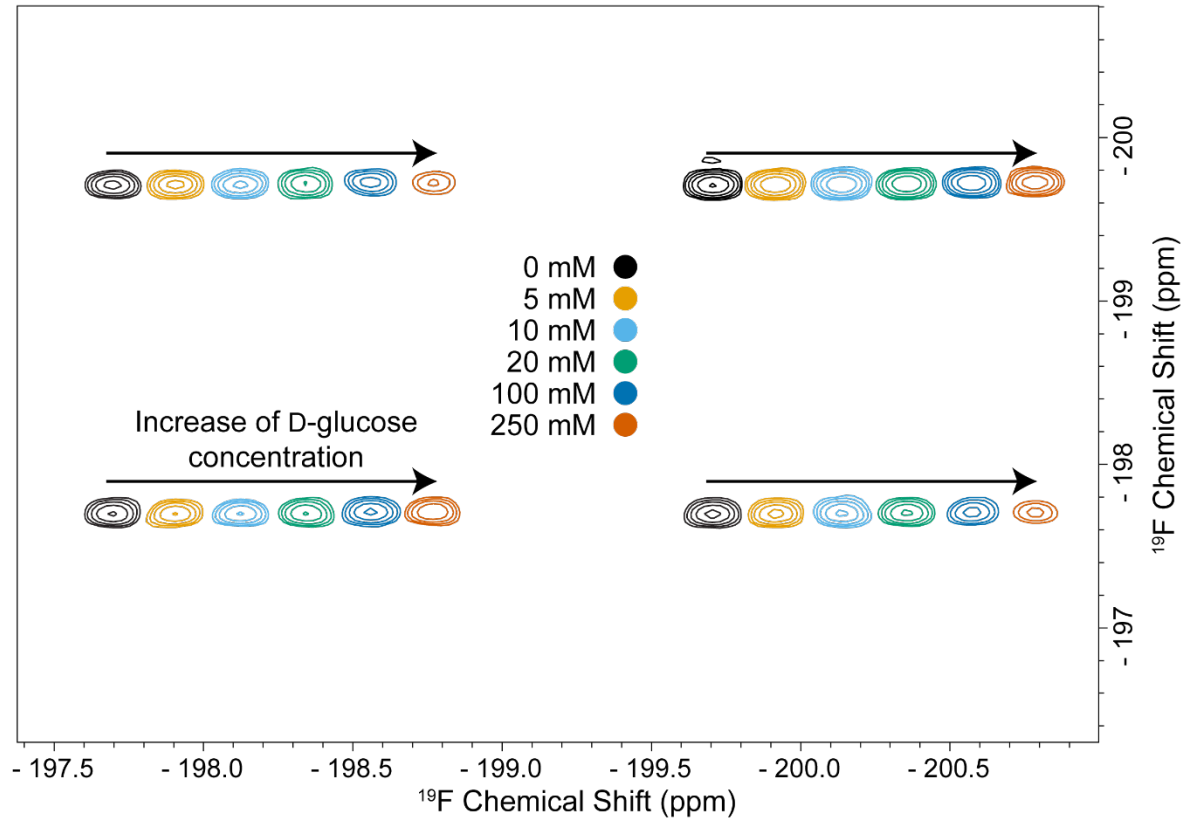

Fig. 7. 2D-EXSY ^{19}F NMR spectra of 10 mM FDG4 in the presence of 0.181 mg mL^{-1} mutarotase and different quantities of D-glucose (0, 5, 10, 20, 100, and 200 mM, as indicated in the figure legend). Mixing time, 2 s. Buffer: 20 mM Na_2HPO_4, 127 mM NaCl, 0.1 mM EDTA, 0.1 mM DTT and 10% D_2O (pH 7.4). For clarity, the spectra (apart from the black one) were shifted horizontally with respect to each other.

As in the previous section, the apparent rate constants of FDG4 anomerisation were estimated from 2D-EXSY spectra of Fig. 7 by the back-transformation procedure (Eq. 8). The estimated values of $k_{\alpha\beta}$ and $k_{\beta\alpha}$ are summarised in Table 3. Initial addition of 5 mM D-glucose to the sample caused a small, non-significant increase in the apparent rate constants; however, further increase in the concentration of D-glucose in the sample led to a steady decline of the $k_{\alpha\beta}$ and

$k_{\beta\alpha}$ values. Upon introduction of 100 mM D-glucose (10-fold excess relative to FDG4), the apparent rate constants were reduced by a factor of ~2, while 250 mM D-glucose (25-fold excess) led to a rate reduction by a factor of ~3.5. This clearly indicated competition of D-glucose with FDG4 for the binding site of the enzyme and suggests that FDG4 could bind to the enzyme in a similar way to its natural substrates.

Table 3. Values of the apparent rate constants $k_{\alpha\beta}$ and $k_{\beta\alpha}$ of 10 mM FDG4 in the presence of 0.181 mg mL^{-1} mutarotase and different concentrations of D-glucose. The values were estimated from the 2D-EXSY spectra of Fig. 7 by the back-transformation procedure.

D-Glucose concentration (mM)	$\boldsymbol{k_{\alpha\beta}}$ **(s^{-1})**	$\boldsymbol{k_{\beta\alpha}}$ **(s^{-1})**
0	0.50 ± 0.01	0.67 ± 0.01
5	0.55 ± 0.02	0.76 ± 0.01
10	0.53 ± 0.03	0.71 ± 0.04
20	0.45 ± 0.02	0.61 ± 0.01
100	0.25 ± 0.01	0.33 ± 0.01
250	0.15 ± 0.01	0.19 ± 0.02

Next, we set out to probe whether the other FDGs, despite the absence of their rapid anomerisation by mutarotase, served as inhibitors of the reaction. We recorded 2D-EXSY spectra of 5 mM FDG4 in the absence and presence of 10-fold excess of each of the other individual sugars. Similarly to D-glucose, at a 10-fold excess in concentration, all tested sugars led to a reduction in the intensity of the FDG4 exchange cross-peaks. The apparent exchange rate constants in the absence ($k^0_{\alpha\beta}$ and $k^0_{\beta\alpha}$) and presence of a 10-fold excess of FDGs ($k_{\alpha\beta}$ and $k_{\beta\alpha}$) from the corresponding 2D-EXSY spectra, led to the ratios $k^0_{\alpha\beta}/k_{\alpha\beta}$ and $k^0_{\beta\alpha}/k_{\beta\alpha}$. These were used as indicators of the inhibitory efficiency of each of the studied F-sugars. The ratios, along with the corresponding value for D-glucose (from Table 3), are summarised in Table 4. FDG2, FDG3 and FDG23 had similar inhibitory efficiency as D-glucose, reducing the anomerisation rate of FDG4 by a factor of ~2. Interestingly, FDG2233 stood out as the most potent inhibitor, reducing the catalytic rate by a factor of ~5 under conditions of similar concentration.

Table 4. Ratios of the apparent rate constants of FDG4 anomerisation in the absence of inhibitors ($k^0_{\alpha\beta}$ and $k^0_{\beta\alpha}$) and in the presence of their 10-fold excess ($k_{\alpha\beta}$ and $k_{\beta\alpha}$). Experiments were carried out in the presence of 5 mM

FDG4 and 0.046 mg mL^{-1} mutarotase, with the exception of those involving competition by D-glucose, which used 10 mM FDG4 and 0.181 mg mL^{-1} mutarotase.

Added sugar	$k^0_{\alpha\beta}/k_{\alpha\beta}$	$k^0_{\beta\alpha}/k_{\beta\alpha}$
D-glucose	2.0 ± 0.1	2.0 ± 0.1
FDG2	1.7 ± 0.1	1.7 ± 0.1
FDG3	2.8 ± 0.6	2.6 ± 1.1
FDG23	2.4 ± 0.2	2.6 ± 0.2
FDG2233	5.4 ± 0.6	5.0 ± 1.2

Discussion

Kinetics

The data of Table 2 and Fig. 6 indicated that the mutarotase activity rose steadily upon increasing its concentration, up to the highest value of 0.174 mg mL^{-1}. The linear model accounted well for the dependence of the apparent rate constants on the concentration of added enzyme ($R^2 = 0.991$ for $k_{\alpha\beta}$ and $R^2 = 0.987$ for $k_{\beta\alpha}$; Fig. 6). This suggests that there was no substantial denaturation of protein in the solution, as any aggregation/precipitation of the protein would lead to a reduction in the increase of $k_{\alpha\beta}$ and $k_{\beta\alpha}$ values upon further additions of the enzyme. As many proteins aggregate at high concentration, it remains to be tested which concentration lead to a plateau in the enzyme activity.

As seen from Figs 3-4, fluorination of the glucose ring at positions 2 or 3 prevented (detectable on the 2-s time scale) mutarotase activity. The fact that, among the five studied fluorinated sugars, only FDG4 displayed rapid anomerisation by mutarotase, was to some extent expected from the substrate selectivity consideration discussed in our previous manuscript (in this Special Edition). Since D-glucose was shown to be an inhibitor of FDG4 anomerisation (Fig. 7, Table 3), the F-sugar putatively interacts with the same or similar (or a subset of them) amino acid residues in the active site of the enzyme as do the natural substrates. Quantification of the anomerisation rates of FDG4 in the absence and presence of other sugars allowed us to establish that FDG2, FDG3, FDG23 and FDG2233 also interact with the mutarotase and act as inhibitors (most likely *competitive* inhibition) of the FDG4 anomerisation. FDG2233, in particular, appears to be a strong inhibitor of mutarotase, reducing the anomerisation rate of FDG4 by a factor ~5 when present at a 10-fold excess concentration; while all other sugars, including D-glucose, reduced the anomerisation rate by a factor in the range 1.7-2.8 under similar conditions

of enzyme and substrate concentration. Although the change of -OH for fluorine obviously impacts on the hydrogen bonding energies, sugar deoxyfluorination leads to an increased hydrophobicity [the log*P* values increase by successive fluorination (FDG2: -2.21, FDG23, -1.11, FDG2233, -0.32)],[29] and the resulting increase in hydrophobic desolvation is expected to benefit binding affinity. In addition, the axial fluorine atoms in FDG2233, which formally replace a weakly polarised C–H bond with a strongly polarised C–F bond, can engage in additional polar interactions, as precedented by the interactions of a tetrafluoronated Gal*p*-UDP derivative with galactose mutase (UGM; EC. 5.4.99.9).[30] These considerations are consistent with the "polar hydrophobicity" effect as advanced by DiMagno et al.[19, 31]

Catalytic mechanism from a structural/chemical perspective

The catalytic mechanism of porcine kidney mutarotase is postulated to be the same as for the enzyme from *L. lactis* (as described in our previous paper in this Special Edition) (Scheme 2).[32] This mechanism hinges on the constellation of four highly-conserved (between reported structures) amino acid residues.[32] Thus, His96 and Asp243 are involved in positioning the pyranose ring in the active site via H-bonding, while Glu304 and His170 are catalytic.[32] The imidazole moiety of His170 is the active-site *acid* that delivers a proton to the C5 oxygen atom (reaction A in Scheme 2); while the carboxylate of Glu304 acts as the active-site *base*, abstracting the proton from the saccharide C1-OH (reaction B in Scheme 2). Overall, these two reactions give rise to ring cleavage and formation of the free aldehyde. Next, a 180° rotation around the C1-C2 bond, followed by abstraction of a proton on the oxygen on C5 by His170 and donation of a proton back from Glu304 to the C1-oxygen, leads to product formation.[32]

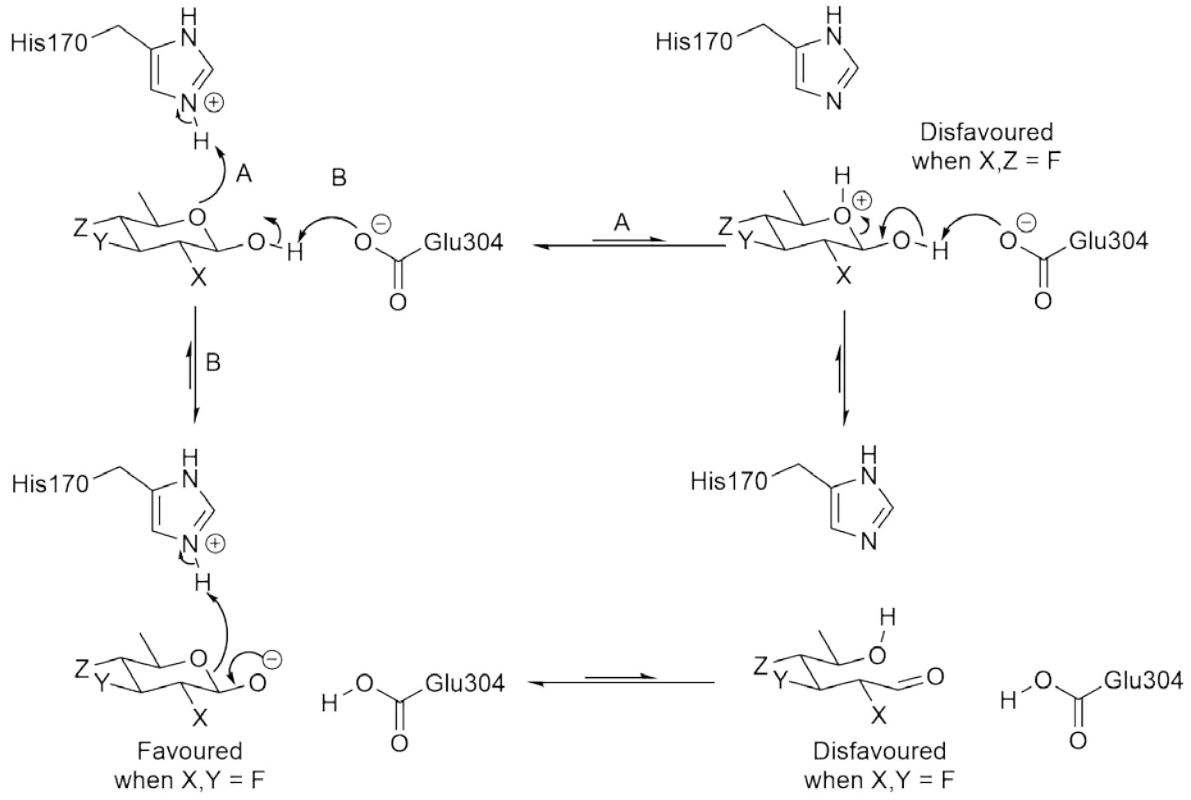

Scheme 2. Individual steps of the mechanism of the anomerisation catalysed by mutarotase, with the influence of fluorine's electron withdrawing effect.

Overall, there are at least three events in the mutarotase-catalysed reaction: (1) binding of the substrate to the enzyme's active site; (2) catalytic acid/base interaction of the enzyme with the substrate to cleave and/or re-link the sugar ring; and (3) rotation around the C1-C2 bond. It is the slowest among these three steps that will be rate-determining for the overall reaction. These three possibilities are analysed next in the context of the experiments conducted here with the F-substituted glucoses.

First, suppose that binding of the substrate to the enzyme determines the overall rate of the reaction. As discussed in detail in previous first manuscript (in this Special Edition), (deoxy)fluorination might potentially enhance/reduce the energy of the hydrogen-bond interaction.[22, 33] However, given that all sugars are inhibitors of FDG4 anomerisation, it is highly unlikely that a compromised binding of these substrates *alone* would lead to the complete absence of any observed anomerisation of these sugars in the presence of mutarotase (on the studied 2-s time scale).

Second, consider the possibility of the catalytic acid/base action of the enzyme being the rate-determining step. In this scenario, the stability of the intermediates in this step of the

mechanism must be considered (Scheme 2). If protonation of O5 is required first (reaction A), leading to a cationic intermediate, this would be destabilised by the electron-withdrawing influence of the F atom(s). Those in positions 2 and 4 are the closest to O5 so they would have the largest destabilising effect on the pyranose ring, thus, at least on a qualitative level, leaving FDG3 (and not FDG4 as observed experimentally) as the best substrate for the reaction. If deprotonation of the anomeric OH occurred first (reaction B), then this would be assisted by F atoms of C2 and/or C3 (lower pK_a),[34] resulting in higher reaction rates for FDG2, FDG3, FDG23, FDG2233 rather than FDG4, which is the opposite of what was observed here (Fig. 3). Thus, overall, considering the results of this study, it is unlikely that the acid/base process is the rate determining step.

Finally, suppose that the rotation around the C1-C2 bond is the rate-determining step. The formation of the free aldehyde form of a monosaccharide, generated in the process of enzyme-mediated anomerisation, will be disfavoured if an F-atom is attached to C2 and/or C3, due to its electron withdrawing effect (Scheme 2). In that case, the free aldehyde would have a very short lifetime that may not be sufficiently long for spontaneous rotation around the C1-C2 bond to occur before the next process takes place. In other words, the free aldehyde form of the sugar would become highly electrophilic due to the F-atoms on C2 and/or C3. This would increase its free energy, resulting in a lower free-aldehyde concentration, thus slowing the overall reaction. This would lead to inhibition of the reaction by FDG2, FDG3, FDG23 and FDG2233. Conversely, an F-atom attached to C4 is too far away from the aldehyde carbon (C1) to have any influence on its reactivity, leading to relatively faster anomerisation of FDG4. This interpretation is consistent with what was observed in the present work (Fig. 3). Thus, results presented here suggest that the rotation around the C1-C2 is the rate-determining step of the overall anomerisation reaction catalysed by mutarotase.

In summary, four out of the five studied FDGs (FDG2, FDG3, FDG23, FDG2233), despite their interactions with the mutarotase, displayed low or no enzyme activity as substrates. In contrast, FDG4 was subjected to rapid anomerisation in the presence of mutarotase. This outcome is consistent with the arguments made above, concerning the stability of the free aldehyde intermediate product in the reaction pathway. Our results, combined with qualitative insights into the catalytic mechanism of the enzyme from previous work in this Special Edition (Scheme 2) suggest that the rotation around the C1-C2 bond is the rate-limiting step of the reaction. In general, our analysis of mutarotase kinetics suggests that it could be part of an emerging understanding that applies to many enzymes.

Conclusions

Using ^{19}F NMR assays of mutarotase activity on fluorinated-glucose analogues, we have shown that fluorination of the glucose ring at positions 2 or 3 prevented mutarotase activity (on the time scale of a few seconds), while fluorination of glucose at position 4 retained a significant rate of anomerisation. Thus, mutarotase was unable to catalyse (*rapid*) conversion between the α- and β-anomers if an F-atom was present in the vicinity of C1 (one to two bonds away), suggesting that the stability of the aldehyde form is the crucial factor that determines the overall rate of the mutarotase-catalysed anomerisation. Control experiments proved that the anomerisation of 4-deoxy-4-fluoro-D-glucose (FDG4) was indeed catalysed by mutarotase, and that glucose, as well as the other fluorinated glucose derivatives, were competing substrates. Interestingly, the tetrafluorinated derivative (FDG2233) was identified as the best inhibitor of the enzyme.

Absence of *rapid* reaction for the four F-glucoses suggests their use in studies of transmembrane exchange *in vivo*, potentially followed by intracellular metabolism. Many enzymes have significant anomeric specificity, thus leaving one of the anomers unreacted in the case of slow anomerisation. This could lead to accumulation of these sugars as probes of intracellular volume in magnetic resonance imaging/spectroscopy experiments, especially of the kidney.

Future directions for the type of NMR analysis used here include the study of a large variety of potential inhibitors of mutarotase by using the FDG4 exchange reaction as the basis for the assay. Perturbation of the exchange rate by other (substituted) saccharides and polyols as in [35] is possible. F-labelled solutes might be used to study saccharide uptake and metabolism in the kidney and other tissues where the enzyme is of high activity, in normal and disease states. Future investigations using F-glucoses will be motivated by questions emerging from cellular and enzyme studies in the field of carbohydrate transport and metabolism.

Materials and methods

Materials

DL-dithiothreitol (DTT) and mutarotase (aldose 1-epimerase; EC. 5.1.3.3) from porcine kidney (suspension in 3.2 M $(NH_4)_2SO_4$, 8200 units per mg of protein, 2.9 mg of protein per mL; one unit increases the spontaneous mutarotation of α-D-glucose to β-D-glucose by 1.0 μmol min^{-1} at pH 7.4 and 25°C) were from Sigma Aldrich (St. Louis, MO, USA). AR grade anhydrous

Na_2HPO_4 was from Ajax Chemicals (Auburn, NSW, Australia). AR grade ethylenediaminetetraacetic acid (EDTA) was from Mallinckrodt (Paris, Kentucky, USA). AR grade NaCl was from APS (Seven Hills, NSW, Australia). D_2O (99.75%) was from the Australian Institute of Nuclear Science and Engineering (Lucas Heights, NSW, Australia).

2-fluoro-2-deoxy-D-glucose (FDG2), 3-fluoro-3-deoxy-D-glucose (FDG3), and 4-fluoro-4-deoxy-D-glucose (FDG4) were purchased from Carbosynth (Compton, UK). 2,3-difluoro-2,3-dideoxy-D-glucose (FDG23) and 2,2,3,3-tetrafluoro-2,3-dideoxy-D-glucose (FDG2233) were synthesised as described previously.[24, 36]

Methods

The buffer for the NMR experiments contained 20 mM Na_2HPO_4, 127 mM NaCl, 0.1 mM EDTA and 0.1 mM DTT, with pH adjusted to 7.4 and measured osmolality of 300 mOsm kg^{-1}. 0.1 mM DTT and 0.1 mM EDTA was required to maintain stability of the mutarotase during the NMR experiments.

Samples were prepared by dissolving the F-sugar(s) in 2.5 mL of the NMR buffer, with addition of 0.2 mL of mutarotase stock solution, and 0.3 mL of D_2O saline [as per [11]]. For the ^{19}F NMR experiments, 0.5 mL of the sample was placed into a 5-mm glass NMR tube and the experiments were recorded at 37°C in a vertical wide-bore 400 MHz (376.5 MHz for ^{19}F) NMR spectrometer (Bruker, Karlsruhe, Germany) using a dual ^{19}F-^{1}H probe and Bruker Topspin 3.2 for spectral acquisition.

The 1D ^{19}F NMR spectra were acquired using a single radio frequency (RF) pulse per free induction decay (FID), using the standard Bruker pulse sequence 'zgig', with ^{1}H WALTZ16 decoupling applied during data acquisition. Each FID consisted of 8192 complex points. The spectral width was 127.729 ppm, with the carrier frequency set to -167 ppm. The ^{1}H decoupler carrier frequency was set to 5 ppm. The FID acquisition time was 170.4 ms. An exponential line-broadening window function of 4 Hz was applied, following by zero-filling to 32768 complex points.

The ^{19}F 2D-EXSY pulse sequence used ^{1}H decoupling in both acquisition dimensions, as described in [22], using a mixing time of 2 s. The ^{1}H decoupler carrier frequency was set to 5 ppm. As is typical for 2D-EXSY experiments, the value of the mixing time had been adjusted in order to extract the maximum amount of information on the exchanging system. Since only cross-peaks for FDG4 were seen (within the levels of detection), the mixing time was adjusted

to maximise the intensity of the cross peaks corresponding to this sugar (2 s). Shorter mixing times led to weak cross-peaks, as only a small extent of reaction had occurred. However, mixing times that were longer led to a decrease of the overall signal-to-noise ratio in the spectrum because of longitudinal relaxation of the magnetisation.

For the 2D-EXSY experiments with FDG2, FDG3, FDG4 and FDG23, two FIDs consisting of 128 complex points were acquired with the inter-transient delay of 8 s, and 64 time increments were applied to record the indirect dimension. The spectral width was 6.5 ppm in both dimensions, with the carrier frequencies set to -197.75 ppm. This resulted in an acquisition time of 52.3 and 13.1 ms in the direct and indirect dimensions, respectively. Both dimensions were multiplied by a cosine-squared bell window function and zero-filled to a matrix of 256 × 256 real points. Forward linear prediction was used in the indirect dimensions with 32 fitted coefficients.

For the 2D-EXSY experiment with FDG2233, two FIDs consisting of 512 complex points were acquired with the inter-transient delay of 2 s, and 256 time increments were applied to record the indirect dimension. The spectral width was 22.065 ppm in both dimensions, with the carrier frequencies set to -130 ppm. This resulted in an acquisition time of 61.6 and 15.4 ms in the direct and indirect dimensions, respectively. Both dimensions were multiplied by a cosine-squared bell window function and zero-filled to a matrix of 1024 × 512 real points. Forward linear prediction was used in the indirect dimensions with 32 fitted coefficients.

The spectra were processed and analysed using Bruker TopSpin 3.5 or 4.0, which involved peak picking and integration of 1D spectra by fitting Lorentzian line shapes. Integration of peaks in the 2D spectra was done using NMRFAM-Sparky[37] by fitting Gaussian shapes. The back-transformation calculations as well as linear model fitting and error analysis were implemented in *Mathematica* 12.0 (Wolfram Research, Champaign, IL, USA).

Acknowledgements

The work was funded by a grant from the Leverhulme Trust (RPG-2015-211) and from the Australian Research Council (DP140102596). Dr Seung Seo Lee, University of Southampton, is thanked for critical and insightful comments on the manuscript; and we thank the University's instrumentation umbrella organisation Sydney Analytical, and Dr Ann Kwan in particular, for the maintenance and supervision of the NMR spectrometers at the University of Sydney.

Conflicts of interest

The authors declare no conflicts of interest.

References

[1] W. Sacks, *Science*. **1967**, *158*, 498.

[2] W. Sacks, *Arch. Biochem. Biophys.* **1968**, *123*, 507.

[3] P. W. Kuchel, B. E. Chapman, J. R. Potts, *FEBS Lett.* **1987**, *219*, 5.

[4] R. Bentley, *Annu. Rev. Biochem.* **1972**, *41*, 953.

[5] D. J. Timson, R. J. Reece, *FEBS Lett.* **2003**, *543*, 21.

[6] H. M. Holden, I. Rayment, J. B. Thoden, *J. Biol. Chem.* **2003**, *278*, 43885.

[7] S. M. Howard, M. R. Heinrich, *Arch. Biochem. Biophys.* **1965**, *110*, 395.

[8] G. G. Bouffard, K. E. Rudd, S. L. Adhya, *J. Mol. Biol.* **1994**, *244*, 269.

[9] A. S. Keston, *Anal. Biochem.* **1964**, *9*, 228.

[10] M. Maebayashi, M. Ohba, T. Takeuchi, *J. Mol. Liq.* **2017**, *232*, 408.

[11] P. W. Kuchel, B. T. Bulliman, B. E. Chapman, *Biophys. Chem.* **1988**, *32*, 89.

[12] I. P. Street, C. R. Armstrong, S. G. Withers, *Biochemistry*. **1986**, *25*, 6021.

[13] C. P. Glaudemans, *Chem. Rev.* **1991**, *91*, 25.

[14] A. Ardá, J. Jiménez-Barbero, *Chem. Commun.* **2018**, *54*, 4761.

[15] J. R. Potts, A. M. Hounslow, P. W. Kuchel, *Biochem. J.* **1990**, *266*, 925.

[16] J. R. Potts, P. W. Kuchel, *Biochem. J.* **1992**, *281*, 753.

[17] R. E. London, S. A. Gabel, *Biophys. J.* **1995**, *69*, 1814.

[18] T. M. O'Connell, S. A. Gabel, R. E. London, *Biochemistry*. **1994**, *33*, 10985.

[19] H. W. Kim, P. Rossi, R. K. Shoemaker, S. G. DiMagno, *J. Am. Chem. Soc.* **1998**, *120*, 9082.

[20] S. Bresciani, T. Lebl, A. M. Z. Slawin, D. O'Hagan, *Chem. Commun.* **2010**, *46*, 5434.

[21] E. Dickinson, J. R. P. Arnold, J. Fisher, *J. Biomol. NMR.* **2017**, *67*, 145.

[22] D. Shishmarev, C. Q. Fontenelle, I. Kuprov, B. Linclau, P. W. Kuchel, *Biophys. J.* **2018**, *115*, 1906.

[23] T. M. O'Connell, S. A. Gabel, R. E. London, *Biochemistry*. **1994**, *33*, 10985.

[24] R. S. Timofte, B. Linclau, *Org. Lett.* **2008**, *10*, 3673.

[25] L. M. McIntyre, D. R. Thorburn, W. A. Bubb, P. W. Kuchel, *Eur. J. Biochem.* **1989**, *180*, 399.

[26] P. W. Kuchel, B. T. Bulliman, B. E. Chapman, G. L. Mendz, *J. Magn. Reson.* **1988**, *76*, 136.

[27] D. Shishmarev, P. W. Kuchel, *Biophys. Rev.* **2016**, *8*, 369.

505 [28] C. L. Perrin, R. K. Gipe, *J. Am. Chem. Soc.* **1984**, *106*, 4036.
506 [29] B. Linclau, Z. Wang, G. Compain, V. Paumelle, C. Q. Fontenelle, N. Wells, et al.,
507 *Angew. Chem. Int. Ed.* **2016**, *55*, 674.
508 [30] K. E. Van Straaten, J. R. Kuttiyatveetil, C. M. Sevrain, S. A. Villaume, J. Jiménez-
509 Barbero, B. Linclau, et al., *J. Am. Chem. Soc.* **2015**, *137*, 1230.
510 [31] J. C. Biffinger, H. W. Kim, S. G. DiMagno, *Chembiochem.* **2004**, *5*, 622.
511 [32] J. B. Thoden, J. Kim, F. M. Raushel, H. M. Holden, *Protein Sci.* **2003**, *12*, 1051.
512 [33] C. Dalvit, A. Vulpetti, *Chem.: Eur. J.* **2016**, *22*, 7592.
513 [34] L. A. Berven, D. H. Dolphin, S. G. Withers, *J. Am. Chem. Soc.* **1988**, *110*, 4864.
514 [35] J. M. Bailey, P. H. Fishman, J. W. Kusiak, S. Mulhern, P. G. Pentchev, *Methods*
515 *Enzymol.* **1975**, *41*, 471.
516 [36] L. Mtashobya, L. Quiquempoix, B. Linclau, *J. Fluor. Chem.* **2015**, *171*, 92.
517 [37] W. Lee, M. Tonelli, J. L. Markley, *Bioinformatics*. **2014**, *31*, 1325.

518